Two-Dimensional Displacement Estimation using Mixed Second-Order Regularization in Total Variation-Based Ultrasound Elastography

Md Ashikuzzaman[1*], Hassan Rivaz[2], and Muyinatu A. Lediju Bell[1,3,4*]

[1]Department of Electrical and Computer Engineering, Johns Hopkins University, Baltimore, MD, USA
[2]Department of Electrical and Computer Engineering, Concordia University, Montreal, QC, Canada
[3]Department of Biomedical Engineering, Johns Hopkins University, Baltimore, MD, USA
[4]Department of Computer Science, Johns Hopkins University, Baltimore, MD, USA

ABSTRACT

A recent technique named Mechanically-inspired $L1$-norm-based Second-Order Ultrasound eLastography ($L1$-MechSOUL) has provided a promising solution to the well-known issue of 2D tracking (both axial and lateral) in ultrasound strain elastography. This technique optimizes a cost function consisting of a data term, a mechanical congruence term, and first- and second-order continuity terms. However, $L1$-MechSOUL's second-order regularizer considers only the unmixed second derivatives and disregards the mixed derivatives, which is a simplification that causes suboptimal noise suppression and inaccurate displacement estimation. We propose to address these challenges by formulating and optimizing a novel $L1$-norm-based second-order regularizer that penalizes both mixed and unmixed displacement derivatives. The unmixed second derivatives in the direction of displacement components (i.e., axial or lateral) regularize the normal strains, whereas we interpret the mixed second derivatives of the axial or lateral displacement to regularize both normal and shear strains. We compared the proposed technique against $L1$-MechSOUL using simulated and phantom datasets, resulting in improved mean structural similarity, elastographic signal-to-noise ratio, and elastographic contrast-to-noise ratio by up to 14%, 91%, and 132%, respectively. These quantitative improvements collectively highlight our ability to deliver high-accuracy 2D displacement and strain estimations that will advance the state-of-the-art in elastography-guided interventions.

Keywords: Ultrasound elastography, two-dimensional tracking, mixed second derivative, noise suppression

1. INTRODUCTION

Quasi-static strain imaging is a mainstream subspecialty of ultrasound elastography,[1–3] which visualizes the strain experienced by a tissue undergoing deformation, assuming that the strain of pathologic tissue will differ from that of healthy tissue. An ultrasound strain elastography pipeline typically comprises radiofrequency (RF) data acquisition pre- and post-tissue deformation, followed by displacement estimation and strain calculations derived from spatial derivatives of the estimated displacement field.

Displacement tracking is arguably the most critical task in ultrasound elastography. Among numerous displacement estimation techniques,[4–9] energy function optimization[10,11] is a two-step solution that offers spatially smooth results. The first step models the tracking problem as a regularized cost function, which is then optimized in the second step. However, like many estimation techniques, energy-based tracking suffers from accuracy challenges associated with the noisy presentation of lateral displacement and strain maps. Mechanically-inspired $L1$-norm-based Second-Order Ultrasound eLastography ($L1$-MechSOUL)[12] was recently developed to address this challenge by utilizing the mechanical relationship driven by the effective Poisson's ratio between axial and lateral strains. The $L1$-MechSOUL cost function consists of data and mechanical constancy terms, and a combination of first- and second-order continuity terms. $L1$-MechSOUL uses only the unmixed second derivatives

*Send correspondence to: mashiku1@jh.edu; mledijubell@jhu.edu

Medical Imaging 2024: Ultrasonic Imaging and Tomography, edited by Christian Boehm, Nick Bottenus,
Proc. of SPIE Vol. 12932, 129320A · © 2024 SPIE · 1605-7422
doi: 10.1117/12.3005693

($\partial_y^2(\cdot)$, $\partial_x^2(\cdot)$) to devise the second-order displacement regularizer. This simplified regularization scheme that disregards the mixed second derivatives ($\partial_{xy}^2(\cdot)$) may lead to suboptimal noise suppression and inaccurate estimations of axial and lateral displacement and strain fields.

Herein, we aim to improve accuracy and suppress noise within $L1$-MechSOUL images by formulating a novel $L1$-norm-based (alternatively known as "total variation") second-order regularizer containing both mixed and unmixed derivatives. Previous work[13] utilized the mixed second derivative in $L2$-norm-based vascular elastography. The current work employs the mixed second derivative in an $L1$-norm-based generalized 2D displacement estimation framework.

2. METHODS

2.1 Displacement Tracking Technique

Our goal is to estimate the 2D displacement field between $I_1(i,j)$ and $I_2(i,j)$, which are two ultrasound RF frames collected before and after tissue deformation, where $1 \leq i \leq m$ and $1 \leq j \leq n$. Dynamic Programming (DP)[14] provides a gross estimate of the axial and lateral displacement fields $a(i,j)$ and $l(i,j)$. $L1$-MechSOUL[12] formulates and optimizes a regularized cost function, C_{l1m}, consisting of data fidelity, spatial continuity, and mechanical constraints to obtain $\Delta a(i,j)$ and $\Delta l(i,j)$, which refine the DP rough estimates:

$$\begin{aligned} C_{l1m}(\Delta a_{1,1},...,\Delta a_{m,n},\Delta l_{1,1},...,\Delta l_{m,n}) =& \|D_I(i,j,a_{i,j},l_{i,j},\Delta a_{i,j},\Delta l_{i,j})\|_2^2 + \gamma\|\partial_y a_{1,j}\|_1 + w_f\alpha_1\|\partial_y a - \epsilon_{\mathbf{a}}\|_1 + \\ & w_f\alpha_2\|\partial_x a - \epsilon_{\mathbf{a}}\|_1 + w_f\beta_1\|\partial_y l - \epsilon_{\mathbf{l}}\|_1 + w_f\beta_2\|\partial_x l - \epsilon_{\mathbf{l}}\|_1 + w_s\alpha_1\|\partial_y^2 a\|_1 + \\ & w_s\alpha_2\|\partial_x^2 a\|_1 + w_s\beta_1\|\partial_y^2 l\|_1 + w_s\beta_2\|\partial_x^2 l\|_1 + \alpha_3\|(\partial_x l)_{i,j} + \nu_{i,j}(\partial_y a)_{i,j}\|_1 \end{aligned} \tag{1}$$

where $D_I(\cdot)$ is a data fidelity term representing the difference between the RF signal amplitude in the pre-deformed image and the warped post-deformed image,[12] $\partial_y(\cdot)$ and $\partial_x(\cdot)$ are the axial and lateral first-order derivatives, respectively, $\partial_y^2(\cdot)$ and $\partial_x^2(\cdot)$ denote the unmixed second-order axial and lateral derivatives, respectively, $\epsilon_{\mathbf{a}}$ and $\epsilon_{\mathbf{l}}$ are the axial and lateral adaptive regularization parameters, respectively, $\nu_{i,j}$ is the effective Poisson's ratio, and γ, w_f, w_s, α_1, α_2, α_3, β_1, and β_2 are tunable parameters. From a mechanical engineering perspective, $\partial_y a$ and $\partial_x l$ refer to axial and lateral normal strains, respectively, and $\partial_x a$ and $\partial_y l$ denote axial and lateral shear strains, respectively.

C_{l1m} considers only the unmixed derivatives to devise the second-order regularizer. Therefore, $L1$-MechSOUL can be prone to suboptimal noise suppression and inaccurate displacement estimation. To address these limitations, we introduce both unmixed ($\partial_y^2(\cdot)$, $\partial_x^2(\cdot)$) and mixed ($\partial_{xy}^2(\cdot)$) second-order displacement derivatives in a novel cost function C_{new}.

$$\begin{aligned} C_{new}(\Delta a_{1,1},...,\Delta a_{m,n},\Delta l_{1,1},...,\Delta l_{m,n}) =& C_{l1m}(\Delta a_{1,1},...,\Delta a_{m,n},\Delta l_{1,1},...,\Delta l_{m,n}) + w_s\alpha_m\|\partial_{xy}^2 a\|_1 + \\ & w_s\beta_m\|\partial_{xy}^2 l\|_1 \end{aligned} \tag{2}$$

where α_m and β_m are tunable weights for the mixed second-order regularizer. Analytic optimization of C_{new} in an iterative fashion estimates $\Delta a(i,j)$ and $\Delta l(i,j)$, which are added to $a(i,j)$ and $l(i,j)$ to obtain the final displacement fields. Spatial differentiation of the final displacement fields renders the strain estimates.

2.2 Validation Datasets and Metrics

A publicly available[15] Field II-simulated[16] phantom containing a hard inclusion (background Young's modulus: 20 kPa, inclusion Young's modulus: 40 kPa, Poisson's ratio: 0.49) was used for *in silico* validation. The simulated parameters included a transducer center frequency of 5 MHz and a sampling rate of 50 MHz. Beamformed RF data were acquired at Johns Hopkins University from a breast phantom (CIRS, Norfolk, VA) containing a stiff inclusion (background Young's modulus: 20 ± 5 kPa, inclusion Young's modulus: at least twice of the background, Poisson's ratio: 0.5). An Alpinion E-cube R12 system connected to an L3-8 probe (transmit frequency: 8.5 MHz, sampling rate: 40 MHz) was utilized to acquire the experimental data.

In addition to visual assessment, the mean structural similarity (MSSIM)[17] was used to compare the strain estimates with simulated ground truth values. Elastographic signal-to-noise ratio (eSNR) and elastographic contrast-to-noise ratio (eCNR) were utilized to quantitatively validate *in silico* and experimental phantom results.

3. RESULTS

Figure 1 shows simulated strain estimation results. $L1$-MechSOUL obtains high-quality results revealing the inclusion in axial and lateral strain images. However, there is also undesirable variability in both the target and the background (relative to the ground truth image). The proposed technique qualitatively reduces this variability, better resembling the ground truth. The MSSIM values reported in Table 1 agree with this qualitative observation. In addition, the proposed method provides eSNR and eCNR improvements as large as 31% when compared to $L1$-MechSOUL.

Figure 2 shows strain estimates obtained with the experimental phantom dataset. Both $L1$-MechSOUL and the proposed technique delineate the stiff inclusion in the axial and lateral strain images. The axial strains are qualitatively less noisy than the lateral strains, which is quantitatively supported by the higher eSNR and eCNR values in Table 2. The $L1$-MechSOUL strain images contain visible noise and spurious edges. The proposed technique leverages the power of mixed second-order continuity to suppress the noise and remove the unwanted edges, preserving the boundary between different tissue types. The associated quantitative results in Table 2 support this qualitative superiority of the proposed algorithm with improvements as large as 132% relative to $L1$-MechSOUL.

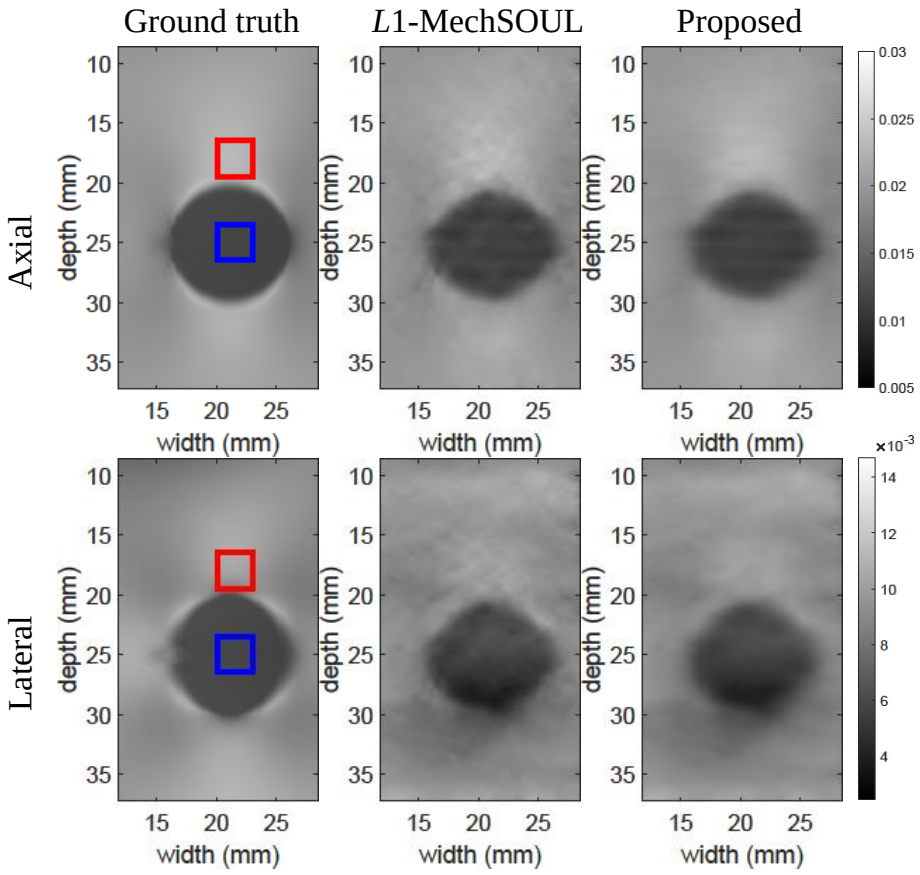

Figure 1: Simulated axial and lateral strain results.

Table 1: MSSIM, eSNR, and eCNR for the simulated dataset.

	MSSIM		eSNR		eCNR	
	Axial	Lateral	Axial	Lateral	Axial	Lateral
$L1$-MechSOUL	0.74	0.50	47.64	53.98	25.82	10.17
Proposed	**0.84**	**0.56**	**62.46**	**67.64**	**33.14**	**11.03**

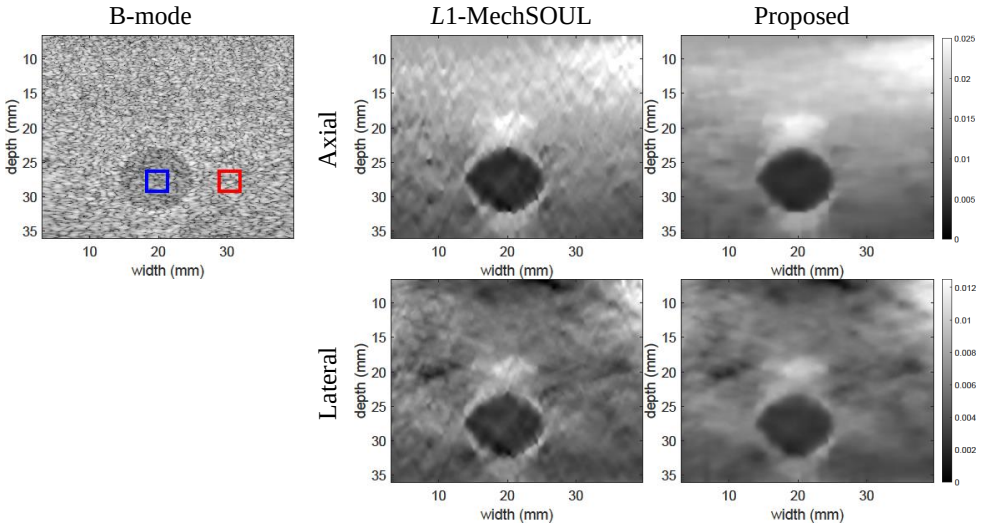

Figure 2: Experimental axial and lateral strain results.

Table 2: eSNR and eCNR for the phantom dataset.

	eSNR		eCNR	
	Axial	Lateral	Axial	Lateral
$L1$-MechSOUL	15.55	12.13	9.70	6.61
Proposed	**29.67**	**16.29**	**22.51**	**11.30**

4. DISCUSSION

This paper proposes a novel two-dimensional displacement estimation method for ultrasound strain elastography that combines unmixed and mixed second-order displacement derivatives in a total variation-based regularization framework. To our knowledge, this work is the first to combine mixed and unmixed second-order regularizers in an $L1$-norm-based 2D displacement tracking algorithm.

Previous work[18] demonstrated that $L1$-norm-based second-order spatial regularization can be an important physics-based modeling component of the cost function associated with an energy function optimization-based displacement tracking algorithm. However, existing $L1$-norm-based speckle tracking techniques[12,18] only consider unmixed derivatives to formulate the second-order regularizer, which underutilizes the full potential of second-order continuity. This work combines mixed and unmixed second derivatives of the displacement fields to ensure multi-directional continuity of axial and lateral strains, leading to improved motion modeling in quasi-static elastography.

Based on the qualitative appearance of axial and lateral strain images (Figures 1 and 2), the proposed algorithm produces smoother axial and lateral strains in both simulated and experimental cases, while maintaining sharp edges. The associated MSSIM (Table 1) demonstrates that the proposed technique produces structurally similar strain images to the ground truth. In addition, SNR and CNR (Tables 1 and 2) demonstrate that the proposed algorithm simultaneously improves noise suppression, while preserving contrast. We also observe that there are some minor discrepancies between the axial and lateral strains (e.g., Figure 2, depth 20 mm, lateral positions 10 mm and 35 mm), which could be either artifacts or indicative of boundary constraints within the experimental phantom. Most importantly, the proposed technique produces high-quality axial and lateral strain estimations, which highlight the strength of the combination of $L1$-norm, mechanical constraints driven by the effective Poisson's ratio, and continuity constraints based on mixed and unmixed second-order derivatives. Future work includes additional phantom acquisitions (e.g., to distinguish potential artifacts from image features indicative of the boundary condition differences), *in vivo* studies, and evaluation of the total strain tensor (axial, lateral, and shear) imaging potential of the proposed displacement tracking technique.

5. CONCLUSION

We present a novel $L1$-norm-based second-order regularizer in a mechanically-inspired 2D displacement estimation framework. The proposed ultrasound strain estimation algorithm exploits both mixed and unmixed displacement derivatives to formulate a second-order regularization scheme. Simulation and phantom validation experiments demonstrated 8-132% improvements in strain estimation quality.

6. ACKNOWLEDGMENT

This work is supported by the National Institutes of Health (NIH) under Award Number NIH R01-EB032960.

References

[1] Ophir, J., Cespedes, I., Ponnekanti, H., Yazdi, Y., and Li, X., "Elastography: A quantitative method for imaging the elasticity of biological tissues," *Ultrasonic Imaging* **13**, 111–34 (1991).

[2] Ashikuzzaman, M., Gauthier, C. J., and Rivaz, H., "Global ultrasound elastography in spatial and temporal domains," *IEEE Transactions on Ultrasonics, Ferroelectrics, and Frequency Control* **66**(5), 876–887 (2019).

[3] Ashikuzzaman, M. and Rivaz, H., "Incorporating multiple observations in global ultrasound elastography," in [*2020 42nd Annual International Conference of the IEEE Engineering in Medicine & Biology Society (EMBC)*], 2007–2010 (2020).

[4] Lediju, M. A., Pihl, M. J., Hsu, S. J., Dahl, J. J., Gallippi, C. M., and Trahey, G. E., "A motion-based approach to abdominal clutter reduction," *IEEE Transactions on Ultrasonics, Ferroelectrics, and Frequency Control* **56**(11), 2437–2449 (2009).

[5] Wen, S., Peng, B., Wei, X., Luo, J., and Jiang, J., "Convolutional neural network-based speckle tracking for ultrasound strain elastography: An unsupervised learning approach," *IEEE Transactions on Ultrasonics, Ferroelectrics, and Frequency Control* (2023).

[6] Pinton, G. F., Dahl, J. J., and Trahey, G. E., "Rapid tracking of small displacements with ultrasound," *IEEE Transactions on Ultrasonics, Ferroelectrics, and Frequency Control* **53**(6), 1103–1117 (2006).

[7] Bell, M. A. L., Byram, B. C., Harris, E. J., Evans, P. M., and Bamber, J. C., "In vivo liver tracking with a high volume rate 4D ultrasound scanner and a 2D matrix array probe," *Physics in Medicine & Biology* **57**(5), 1359 (2012).

[8] Tehrani, A. K., Ashikuzzaman, M., and Rivaz, H., "Lateral strain imaging using self-supervised and physically inspired constraints in unsupervised regularized elastography," *IEEE Transactions on Medical Imaging* **42**(5), 1462–1471 (2022).

[9] Ashikuzzaman, M., Sadeghi-Naini, A., Samani, A., and Rivaz, H., "Combining first-and second-order continuity constraints in ultrasound elastography," *IEEE Transactions on Ultrasonics, Ferroelectrics, and Frequency Control* **68**(7), 2407–2418 (2021).

[10] Ashikuzzaman, M., Hall, T. J., and Rivaz, H., "Incorporating gradient similarity for robust time delay estimation in ultrasound elastography," *IEEE Transactions on Ultrasonics, Ferroelectrics, and Frequency Control* **69**(5), 1738–1750 (2022).

[11] Ashikuzzaman, M., Hall, T. J., and Rivaz, H., "Adaptive data function for robust ultrasound elastography," in [*2020 IEEE International Ultrasonics Symposium (IUS)*], 1–4 (2020).

[12] Ashikuzzaman, M., Tehrani, A. K., and Rivaz, H., "Exploiting mechanics-based priors for lateral displacement estimation in ultrasound elastography," *IEEE Transactions on Medical Imaging* **42**(11), 3307–3322 (2023).

[13] Li, H., Porée, J., Chayer, B., Cardinal, M.-H. R., and Cloutier, G., "Parameterized strain estimation for vascular ultrasound elastography with sparse representation," *IEEE Transactions on Medical Imaging* **39**(12), 3788–3800 (2020).

[14] Rivaz, H., Boctor, E., Foroughi, P., Zellars, R., Fichtinger, G., and Hager, G., "Ultrasound elastography: A dynamic programming approach," *IEEE Transactions on Medical Imaging* **27**(10), 1373–1377 (2008).

[15] Tehrani, A. K. and Rivaz, H., "Displacement estimation in ultrasound elastography using pyramidal convolutional neural network," *IEEE Transactions on Ultrasonics, Ferroelectrics, and Frequency Control* **67**(12), 2629–2639 (2020).

[16] Jensen, J., "Field: A program for simulating ultrasound systems," *Medical & Biological Engineering & Computing* **34**, 351–352 (1996).

[17] Wang, Z., Bovik, A. C., Sheikh, H. R., and Simoncelli, E. P., "Image quality assessment: From error visibility to structural similarity," *IEEE Transactions on Image processing* **13**(4), 600–612 (2004).

[18] Ashikuzzaman, M. and Rivaz, H., "Second-order ultrasound elastography with $l1$-norm spatial regularization," *IEEE Transactions on Ultrasonics, Ferroelectrics, and Frequency Control* **69**(3), 1008–1019 (2022).